Electric Power Systems Research 117 (2014) 21–26

Contents lists available at ScienceDirect

Electric Power Systems Research

journal homepage: www.elsevier.com/locate/epsr

A novel method for locating faults on distribution systems

Yuan Liao*

Department of Electrical and Computer Engineering, University of Kentucky, Lexington, KY 40506, USA

ARTICLE INFO

Article history:
Received 25 April 2014
Received in revised form 22 July 2014
Accepted 23 July 2014

Keywords:
Distribution systems
Fault location
Power system protection
Non-radial distribution systems
System restoration
Feeder shunt capacitances

ABSTRACT

Accurate location of faults in an electric power distribution system is important in maintaining system reliability. Diverse methods have been proposed in the past, which usually have different assumptions and thus are applicable to specific circumstances. This paper attempts to put forth a novel, general fault location method that is applicable to distribution networks with unbalances and multi-sources by employing voltages and currents at the local substation. The method considers feeder shunt capacitances and is applicable to both overhead and underground networks. The method does not require the fault type to be known, and is applicable to any type of faults. The method is based on bus impedance matrix that enables the establishment of the equations governing the relationship of the measurements and the fault location. Evaluation studies have demonstrated the effectiveness of the proposed method and its robustness with respect to potential measurement errors and load variations.

1. Introduction

Accurate location of faults in electric power distribution systems plays an essential role in system restoration and reliability improvement [1–3]. Significant efforts have been spent in the past for developing various types of fault location methods.

A method based on voltage sag data is proposed in [4] to pinpoint the fault location without considering fault resistances. The authors of [5] design an algorithm that makes use of superimposed quantities and iteratively estimates equivalent admittance matrices at both sides of the assumed faulted section. Voltage sag data are harnessed in [6] to locate the fault with the aid of iterative short circuit studies, with the assumption that the fault occurs on a node. In [7], fault location is identified by comparing feeder currents at different sections, where available data may be captured from various automation devices. Utilization of local measurements and network data to find the fault location is discussed in [8]. Ref. [9] derives the fault location by calculating the apparent impedance, and the load is represented by equipment impedance. Measurements from power quality meters are exploited to determine the fault location in [10], where the fault location is estimated through iterative simulation studies. A method for radial systems is described in [11] with suggested ways of ranking possible multiple fault location estimates. The fault-path-current concept is proposed in [12], and iterative short circuit studies are carried out to match the actual measurements. Employment of circuit analysis is expounded in [13–15] to simplify the fault location process. However voltages and currents for the assumed faulted feeder section still need to be iteratively computed. A fault location method is elaborated in [16] based on the principle that system parameters may experience steep changes due to a fault. An approach for trimming down multiple possible fault location estimates due to presence of laterals is provided in [17]. To eliminate or reduce the need of iterative short circuit analysis and iterative voltage and current updates, methods based on direct short-circuit analysis are proposed in [18]. In [19], a method is proposed based on local measurements, which assumes the fault type is provided and is applicable to radial distribution systems.

For underground distribution feeders, fault location poses extra challenges due to presence of large shunt capacitances of cables, ignorance of which may lead to tangible fault location errors [20,21]. A method based on distributed parameter line model by assuming the system is balanced is presented in [20]. Ref. [21] tackles this problem by iteratively compensating the effects of shunt capacitances. These methods are applicable to radial distribution systems. Article [22] presents a two-terminal fault location method for lines little longer than half-wavelength. A method for locating faults on transmission lines using voltage and current at a single bus is described in [23].

Although there exist various fault location methods for transmission lines [24–27], such techniques are generally not applicable to distribution systems since distribution systems are usually unbalanced and are equipped with very few recording devices, usually located at the main substation.

* Tel.: +1 859 257 6064; fax: +1 859 257 3092.
E-mail addresses: yliao@engr.uky.edu, yliaouk@gmail.com

http://dx.doi.org/10.1016/j.epsr.2014.07.026
0378-7796/

This paper aims to propose a general fault location method that is applicable to radial systems or multi-source systems with unbalances, and considers feeder shunt capacitances. The new method obviates the demand for the fault type information and provides a solution for any type of fault, which eliminates errors due to possible fault type misidentification [1,28].

The proposed methods assume that the distribution system network parameters and topology are known, and are based on fundamental frequency phasors. The proposed methods fully model each section of the feeder, and are applicable to non-homogenous feeder that may have varied parameters for each feeder section.

In the rest of the paper, Section 2 presents the new fault location method. Evaluation studies based on simulated data are reported in Section 3, followed by the conclusion.

2. Proposed new fault location method

Fig. 1 depicts a typical power distribution system, including unbalanced loads, a remote source, and main feeders and laterals, which can be overhead or underground cables. For such a system, the following sections present the novel fault location method.

The proposed fault location method is applicable to any type of faults, including single line to ground faults (LG), line to line faults (LL), line to line to ground faults (LLG), three phase faults (LLL) and three phase to ground faults (LLLG) [18].

Existing fault location approaches need to first identify the fault type or assume the fault type to be already decided by another program, and then derive the formula for each type of fault. Erroneous identification of the fault type will lead to wrong fault location calculation. Hence this work will develop a general method that does not need to identify the fault type and thus eliminates the potential error due to fault type misidentification.

2.1. Basic idea of the fault location method

The proposed method is based on bus impedance matrix concept. The voltage and current quantities at any bus during the fault can be expressed in terms of the bus impedance matrix of the faulted network, which is a function of the fault location. The given measurements at the local substation, and the voltages and currents at the fault point can be written in terms of the fault location. Since the fault resistances only consume real power, the imaginary power consumed by fault resistances will be zero. The fault location can thus be obtained.

To cope with intrinsic unbalances, the distribution system will be represented in the three-phase domain, and the phase-domain short circuit analysis technique will be harnessed to derive the fault location. Therefore, the proposed method will naturally accommodate any unbalance in the system. The method will be applicable to non-radial networks.

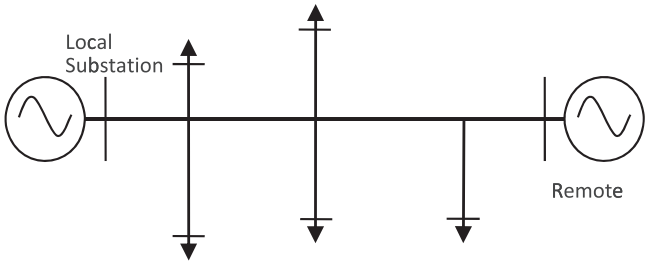

Fig. 1. A sample power distribution system.

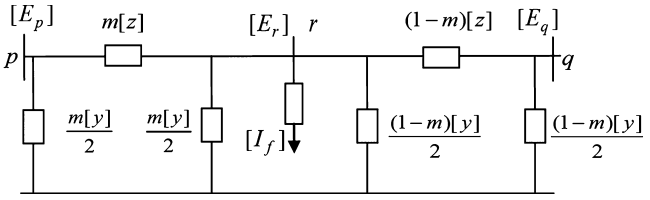

Fig. 2. A section of a power distribution system.

2.2. Derivation of transfer and driving point impedance

Fig. 2 shows the one-line diagram of a section of a distribution system, where a three-phase feeder is assumed. Note that the remaining part of the distribution system is not shown. The following notations are adopted:

$[\cdot]$: designation of a matrix or vector;
n: the total number of nodes of the entire distribution system without counting fault nodes r_1, r_2, and r_3. Note that a node corresponds to a single phase. A three-phase bus consists of 3 nodes, and a two-phase bus has 2 nodes, etc.
p, q: buses of the sample feeder. Bus p comprises nodes p_1, p_2 and p_3, and bus q includes nodes q_1, q_2, and q_3;
r: fault bus, containing nodes r_1, r_2, and r_2;
$[E_p]$: node voltage vector, $[E_p] = [E_{p1},E_{p2},E_{p3}]^T$, with T symbolizing vector/matrix transpose. E_{p1}, E_{p2} and E_{p3} are voltages at node p_1, p_2, and p_3, respectively;
$[E_q]$: node voltage vector, $[E_q] = [E_{q1},E_{q2},E_{q3}]^T$. E_{q1}, E_{q2} and E_{q3} are voltages at node q_1, q_2, and q_3, respectively;
$[E_r]$: node voltage vector, $[E_r] = [E_{r1},E_{r2},E_{r3}]^T$. E_{r1}, E_{r2} and E_{r3} are voltages at node r_1, r_2, and r_3, respectively;
$[I_f]$: fault current through fault resistances, $[I_f] = [I_{f1},I_{f2},I_{f3}]^T$. I_{f1}, I_{f2}, and I_{f3} are fault currents for phase 1, 2 and 3, respectively;
$[z]$: the total series impedance matrix of the feeder, with a dimension of 3 by 3;
$[y]$: the total shunt admittance matrix of the feeder due to shunt capacitances, with a dimension of 3 by 3;
m: per unit fault distance from bus p to the fault point;
$[Z_0]$: the bus impedance matrix of the entire pre-fault distribution system in phase domain, excluding fictitious nodes r_1, r_2, and r_3. $[Z_0]$ will be of size n by n;
$[Z]$: the bus impedance matrix in phase domain of the entire distribution system including the fictitious fault nodes. $[Z]$ will be of size $(n+3)$ by $(n+3)$;
Z_{kl}: the element in the kth row and lth column of $[Z]$;

In implementation, the fault nodes are numbered as follows: $r_1 = n+1$, $r_2 = n+2$, and $r_3 = n+3$.

Matrix $[Z_0]$ can be readily developed. It can be shown that the first n rows and n columns of $[Z]$ are identical to $[Z_0]$, and the other rows and columns of $[Z]$ consist of transfer and driving point impedances related to the fault nodes. The transfer and driving point impedance of $[Z]$ related to the fault nodes can be obtained as

$$[Z_{kr}] = [w]^{-1}\left(\frac{[Z_{kp}]}{m} + \frac{[Z_{kq}]}{1-m}\right) \tag{1}$$

$$[Z_{rr_i}] = [w]^{-1}\left(\frac{[Z_{pr_i}]}{m} + \frac{[Z_{qr_i}]}{1-m} + [z][u_i]\right), \quad i = 1, 2 \text{ or } 3 \tag{2}$$

$$[w] = \frac{[z][y]}{2} + \frac{[u]}{m(1-m)} \tag{3}$$

where $[Z_{kr}]$ is the transfer impedance between node k and fault nodes; $[Z_{rr_i}]$ is the driving point and transfer impedance related to

fault nodes; $[u]$ is the a three by three identity matrix, whose ith column is denoted by $[u_i]$.

It is noted that the above equations hold for a single-phase, two-phase or three-phase feeder, where applicable. The key point is that the transfer and driving point impedances are expressed as functions of the fault location.

2.3. Derivation of fault location

Without losing generality, a fault that occurs on a three phase feeder is examined. Again, no fault type is assumed. Based on the superimposition theory and the meaning of the transfer impedance, the voltage change due to the fault, or superimposed voltage at any bus k can be written as

$$[\Delta E_k] = -[Z_{kr}][I_f] \tag{4}$$

where

$$[\Delta E_k] = [\ \Delta E_{k_1} \quad \Delta E_{k_2} \quad \Delta E_{k_3}\ ]^{\mathrm{T}} \tag{5}$$

$$[Z_{kr}] = \begin{bmatrix} Z_{k_1r_1} & Z_{k_1r_2} & Z_{k_1r_3} \\ Z_{k_2r_1} & Z_{k_2r_2} & Z_{k_2r_3} \\ Z_{k_3r_1} & Z_{k_3r_2} & Z_{k_3r_3} \end{bmatrix} \tag{6}$$

$$[I_f] = [\ I_{f_1} \quad I_{f_2} \quad I_{f_3}\ ]^{\mathrm{T}} \tag{7}$$

$[\Delta E_k]$ is the superimposed voltage at bus k, i.e., the difference between the voltage during the fault and the prefault voltage. Bus k is assumed to consist of nodes k_1, k_2, and k_3. In practice, only the existent nodes will appear in the equation.

It follows from (4) that

$$[I_f] = -([Z_{kr}]^{\mathrm{T}}[Z_{kr}])^{-1}([Z_{kr}]^{\mathrm{T}}[\Delta E_k]) \tag{8}$$

The voltage at the fault nodes during the fault is given by

$$[E_r] = [E_{r0}] - [Z_{rr}][I_f] \tag{9}$$

where

$$[E_r] = [\ E_{r_1} \quad E_{r_2} \quad E_{r_3}\ ]^{\mathrm{T}} \tag{10}$$

$$[E_{r0}] = [\ E_{r_1 0} \quad E_{r_2 0} \quad E_{r_3 0}\ ]^{\mathrm{T}} \tag{11}$$

$$[Z_{rr}] = \begin{bmatrix} Z_{r_1r_1} & Z_{r_1r_2} & Z_{r_1r_3} \\ Z_{r_2r_1} & Z_{r_2r_2} & Z_{r_2r_3} \\ Z_{r_3r_1} & Z_{r_3r_2} & Z_{r_3r_3} \end{bmatrix} \tag{12}$$

$[E_r]$ and $[E_{r0}]$ are the voltages at the fault nodes during the fault and preceding the fault, respectively.

The prefault voltages at the fault nodes can be expressed in terms of the fault location and the prefault node voltages at bus p and q as follows:

$$[E_{r0}] = [w]^{-1}\left(\frac{[E_{p0}]}{m} + \frac{[E_{q0}]}{1-m}\right) \tag{13}$$

where $[E_{p0}]$ and $[E_{q0}]$ are the prefault voltage vectors at respective nodes, which can be estimated utilizing prefault voltages and currents at the substation and the feeder and load impedance, or directly obtained from measuring devices if available.

Based on (8), the complex power consumed by the fault resistances is calculated as

$$S = -[E_r]^{\mathrm{T}}\{([Z_{kr}]^{\mathrm{T}}[Z_{kr}])^{-1}([Z_{kr}]^{\mathrm{T}}[\Delta E_k])\}^{*} \tag{14}$$

where "*" denotes complex conjugate. The fault resistances only consume real power, so the imaginary part of S is zero

$$\mathrm{Imag}(S) = 0 \tag{15}$$

where Imag$(\cdot)$ yields the imaginary part of its argument.

It is seen from (1)–(4), (9) and (13), Eq. (15) has one unknown variable m, which can be determined by the Newton–Raphson technique. It is clearly manifested that fault type information is not needed. It is also noted that the method does not assume fault resistances between phases to be equal; it automatically takes into account unequal fault resistances between phases.

To mitigate impacts of load variations, a load compensation technique is used [5]. The basic idea is to calculate the load level based on measured prefault voltages and currents at the substation, and then scale the static load impedance accordingly. The effectiveness of the method is illustrated in the evaluation study section.

2.4. Ranking of multiple fault location estimates

Multiple possible fault location estimates may result from the proposed method due to presence of laterals when using the local measurements. Ranking of multiple estimates is discussed in this section based on fault boundary conditions.

Once the fault location is estimated, the fault current flowing through the fault resistances can be calculated using (8). Because the healthy phase has a zero fault current, the fault type can then be easily identified below. If the calculated fault current of a phase exceeds the prescribed threshold value, that phase will be considered a faulted phase; the threshold value is chosen as 1 A in this study. The sum of the fault currents is calculated, and a non-zero value indicates a ground fault. Since the fault current at the fault point is directly used, this fault type classification method is not affected by load current, and thus this method may be more accurate than that based on voltages and currents at the substation.

In case of multiple fault location estimates, a similar method to [19] is applied to rank the estimates. For faults involving one or two phases, based on the fault location estimate, the sum of the magnitude of the calculated fault currents of the non-faulted phases is obtained. For example for a BG fault on a three phase feeder, the value is obtained as

$$I_{err} = |I_{fA\_cal}| + |I_{fC\_cal}| \tag{16}$$

where I_{err} stands for the mismatch current, I_{fA_cal} is calculated phase A fault current, and I_{fC_cal} denotes calculated phase C fault current.

For phase to phase faults, an additional index is calculated. Take a BC fault as an example, the value is calculated as

$$I_{errLL} = |I_{fB\_cal} + I_{fC\_cal}| \tag{17}$$

where I_{fB_cal} denotes calculated phase B fault current.

For three phase faults, the following quantity is calculated:

$$I_{err} = |I_{fA\_cal} - I_{fB\_cal}| + |I_{fB\_cal} - I_{fC\_cal}| + |I_{fC\_cal} - I_{fA\_cal}| \tag{18}$$

The smaller the calculated value, the higher the according fault location is ranked, and the more likely the fault location is the true one. It will be shown that the ranking method may not work for three phase faults with unequal fault resistances. Also, note that a negative value of the complex power S will indicate a fake estimate.

Understandably, it may not always be possible to distinguish between some estimates depending on network structure and parameters. For example, it is not possible to tell apart two faults that fall on two identical feeder laterals, respectively, if only the local measurements are available. However, the ranking method may eliminate some fake estimates.

The application of the proposed fault location method is illustrated as follows. The proposed method can be integrated into the Energy Management System and Supervisory Control and Data Acquisition System. In this way, the fault location module will have access to the most updated network topology. The bus impedance

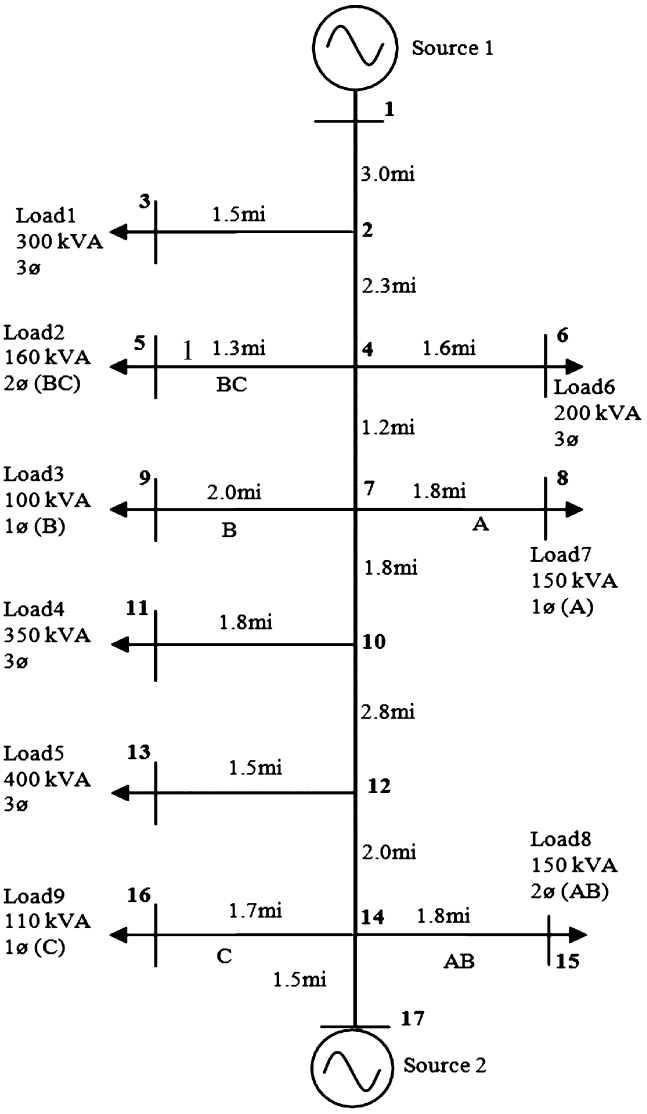

Fig. 3. The power distribution system used in evaluation studies.

matrix of the network is then developed. Then the fault location method as presented in Section 2.3 is applied to find out a list of fault location estimates. Then the approach in Section 2.4 is applied to eliminate fake estimates. Again, it is noted that it may not always be possible to eliminate all fake estimates.

3. Evaluation studies

This section presents the results based on simulation studies for evaluating the developed fault location algorithms. Matlab SimPowerSystems has been utilized to generate transient waveforms for faults of different types, locations and fault resistances [29]. Fast Fourier Transform (FFT) is then harnessed to calculate the required voltage and current phasors, which are fed into the developed algorithms to obtain the fault location. Shunt capacitances of feeders are modeled using nominal PI method. Fig. 3 portrays a sample 12.47 kV underground power distribution system, which will be utilized in the study [18].

This system includes three-phase, two-phase and one-phase laterals and loads. For example, load 7 is a phase A load and is supplied by a single-phase lateral tap from the main feeder. The lengths of feeders in miles, and the load ratings and phases are labeled. A power factor of 0.9 is assumed for all the nine loads.

Table 1
Fault location estimates yielded by the proposed algorithm.

Faulted section	Fault type	FL (p.u.)	Fault res. (Ω)	FL esti. err. (%)
1–2	LG	0.3	50	0.02
	LL	0.5	10	0.00
	LLG	0.7	[1,2,10]	0.00
	LLL	0.7	[1,1,1]	0.00
	LLLG	0.6	[1,1,1,5]	0.00
4–7	LG	0.4	50	0.09
	LL	0.7	5	0.01
	LLG	0.5	[1,1,10]	0.01
	LLL	0.6	[1,1,1]	0.01
	LLLG	0.8	[1,2,3,50]	0.02
7–9	LG	0.5	100	0.01
10–11	LG	0.9	50	0.02
	LL	0.5	1	0.01
	LLG	0.4	[1,1,50]	0.01
	LLL	0.9	[5,5,5]	0.01
	LLLG	0.6	[1,1,1,5]	0.01
14–15	LG	0.7	0	0.00
	LG	0.7	50	0.03
	LL	0.7	10	0.04
	LLG	0.3	[1,1,30]	0.07

Single- or double-phase laterals are indicated, while others are of three phases. The feeder series impedance and shunt admittance data are referred to [30].

The developed algorithm has been implemented in Matlab. In the study, a starting value of 0.5 p.u. for fault location is utilized, and all the cases converged within 10 iterations. The estimation accuracy is measured by the percentage error calculated as

$$\%\text{error} = \frac{|\text{Actual location} - \text{Estimated location}|}{\text{Total length of the main feeder}} \times 100 \qquad (19)$$

Different types of faults with various locations, from 0.1 to 0.9 p.u. on each segment of the feeder, and diverse fault resistances, from 1 to 100 Ω for grounded faults and from 1 to 10 Ω for non-grounded faults, have been studied and typical results are presented in this section.

Table 1 presents the fault location estimates obtained by the proposed method. In Table 1, columns 1–4 list the faulted section, fault type, actual fault location and fault resistance, respectively. The fault location error reached by the new method is given in columns 5. Fault location is measured from the beginning bus of the line section. It is noted that the developed method is able to automatically handle cases with unequal fault resistances between phases, which are listed separately. For example, in the 3rd case, the actual inter-phase fault resistances are 1.00 and 2.00 Ω, and the ground fault resistance is 10.00 Ω. It is revealed that quite accurate results for fault location have been achieved by the developed algorithm. Note that for the case where a LG fault occurs on section 14–15 with zero fault resistance, analytical short-circuit analysis is used to generate the fault data to test the algorithm, since the simulation software does not allow a zero valued fault resistance.

Presence of laterals may cause multiple estimates. The process described in Section 2.4 for ranking fault estimates is illustrated below.

Case 1: For an AG fault, designated as [4–7, 0.3], which falls on line 4–7, 0.3 p.u., with fault resistance 1.0 Ω, two fault location estimates are obtained:

[4–7, 0.2993], the mismatch current I_{err} = 0.0248, and
[4–6, 0.1487], the mismatch current I_{err} = 9.919.

Since 0.0248 is smaller than 9.919, the solution [4, 7, 0.2993] is regarded as the most likely solution, which is correct.

Table 2
Impacts of measurement errors on fault location estimates.

Fault type	Fault res. (Ω)	FL (p.u.)	Fault location estimation error (%)			
			With 1% cur. error	With 2% cur. error	With 1% cur. and vol. error	With 2% cur. and vol. error
LG	100	0.2	0.48	0.96	0.97	2.00
LL	1	0.5	0.64	1.29	1.28	2.58
LLG	[1,1,50]	0.8	0.70	1.41	1.40	2.82
LLL	[5,5,5]	0.7	0.82	1.65	1.64	3.33
LLLG	[1,1,1,10]	0.6	0.66	1.34	1.32	2.67

Table 3
Impacts of load variations on fault location estimates (without load compensation).

Fault type	Fault res. (Ω)	FL (p.u.)	Fault location estimation error (%)		
			With 5% load var.	With 10% load var.	With 20% load var.
LG	1	0.7	0.08	0.13	0.24
LG	50	0.7	2.44	5.00	10.5
LL	5	0.7	0.07	0.14	0.27
LLG	[1,1,10]	0.6	0.07	0.11	0.18
LLL	[1,1,1]	0.5	0.06	0.08	0.12
LLLG	[1,1,1,10]	0.5	0.06	0.08	0.13

Case 2: For an ABC fault [4–7, 0.45], with fault resistances of 1 Ω, two estimates are obtained:

[4–7, 0.4491], I_{err} = 212.25, and [4–6, 0.2377], I_{err} = 214.12.

The results indicate that the most likely fault location is [4–7, 0.4491], which is correct.

However, as pointed in Section 2.4, for an ABC fault with unequal fault resistances, the correct estimate may be misidentified, as demonstrated in Case 3.

Case 3: For an ABC fault [4–7, 0.45], with unequal fault resistances of 1, 2 and 5 Ω, two estimates are obtained:

[4–7, 0.4490], I_{err} = 708.02, and [4–6, 0.2247], I_{err} = 693.76.

The results indicate that the most likely fault location is [4–6, 0.2247], which is incorrect. However, both solutions will lead to the same voltages and currents at the substation based on short circuit studies. Therefore, both solutions indeed satisfy the measurements. This indicates that using only the substation measurements cannot distinguish between the two fault points; additional information must be available so as to tell apart the two points.

Case 4: In another example, for a BC fault [4–7, 0.30], with fault resistance of 1 Ω, three estimates are obtained:

[4–7, 0.2991], I_{err} = 0.0042, I_{errLL} = 0.0014
[4–6, 0.1600], I_{err} = 1.3455, I_{errLL} = 0.4632, and
[4–5, 0.1857], I_{err} = N/A, I_{errLL} = 1.3357.

Since lateral 4–5 only contains BC phases, only I_{errLL} is calculated. So, using the value of I_{errLL}, the fault locations are ranked in order of likelihood as: [4,7, 0.2991], [4–6, 0.1600], 4–5, 0.1857]. So, the most likely fault location is [4–7, 0.2991], which is the correct result.

However, in some instances, it may be impossible to distinguish between some faults as shown in the following case.

Case 5: For instance, for a BCG fault [4–7, 0.30], with fault resistance of 1 Ω, three estimates are obtained:

[4–7, 0.2991], I_{err} = 0.0111; [4–6, 0.1512], I_{err} = 3.4475; and [4–5, 0.1669], I_{err} = N/A.

Although [4–7, 0.2991] can be ranked higher than [4–6, 0.1512], the third solution [4–5, 0.1669] cannot be ranked, since feeder section 4–5 only has BC phases and does not have a healthy phase. So, there will be at least two possible estimates: [4–7, 0.2991] and [4–5, 0.1669]. In such cases, the two fault locations are indistinguishable based only on substation measurements.

In addition, the research also examines the impacts of possible measurement errors on fault location estimates. Table 2 shows the fault location estimates under various errors in current measurements for faults occurring on feeder section 2–4. The first three columns list actual fault type, fault resistance and fault location. Columns 4 and 5 display fault location estimates for cases with 1% and 2% errors in current measurements, respectively. All the current measurements are either increased or decreased together by the specified error, and the larger fault location error is shown. The effects of inaccuracy in voltage measurements have also been studied, and results similar to columns 4 and 5 have been observed, which are not shown here. Columns 6 and 7 present results when there are errors in current and voltage measurements simultaneously; errors of opposite sign are imposed on current and voltage measurements, since errors of the same sign would have no impacts on fault location estimate. It is evinced that the fault location estimates are quite robust to errors in current and voltage measurements.

The proposed algorithms utilize equivalent impedance model for load obtained at nominal conditions, and load variation may cause errors in fault location estimates. As examples, Table 3 presents fault location estimates for faults occurring on feeder section 4–7 with various load variations being imposed. The first three columns list the actual fault type, fault resistance and fault location, respectively. The remaining three columns give the fault location error corresponding to 5%, 10% and 20% load variations, respectively. It is shown that the fault location estimates for LG faults degrade more due to load variations when the fault resistance increases. For LG faults, since increased fault resistance leads to smaller fault currents, load accuracy plays a bigger role in determining fault location, and thus has a larger impact on fault location accuracy. The fault location estimates for other types of faults are desirably insensitive to load variations.

To mitigate the impact of load variations, a method similar to that proposed in [5] has been utilized to compensate load variations. The measured prefault voltages and currents at the local substation are utilized to adjust the load impedance [18]. The following section demonstrates the effectiveness of this technique. The power contribution factor of the remote source is assumed to be a constant. Table 4 shows four cases of individual load variations. In the first two cases, the load is decreased by an average of 20% and

Table 4
Individual load variations (%).

Case #	Load #								
	1	2	3	4	5	6	7	8	9
1	−15	−25	−30	−10	−15	−25	−15	−30	−15
2	−40	−15	−25	−40	−20	−35	−40	−25	−30
3	15	25	30	10	15	25	15	30	15
4	40	15	25	40	20	35	40	25	30

Table 5
Effectiveness of adopted load compensation technique for fault location.

Fault type	Fault res. (Ω)	FL (p.u.)	Fault location estimation error (%)			
			Case 1 (−20% load var.)	Case 2 (−30% load var.)	Case 3 (20% load var.)	Case 4 (30% load var.)
LG	50	0.7	0.43	0.59	0.52	1.32
LL	5	0.7	0.05	0.14	0.09	0.07
LLG	[1,1,10]	0.6	0.05	0.05	0.04	0.06
LLL	[1,1,1]	0.5	0.05	0.04	0.03	0.05
LLLG	[1,1,1,10]	0.5	0.04	0.04	0.04	0.05

30%, respectively. The load is increased by an average of 20% and 30% respectively in the last two cases.

The load compensation technique has been shown to be quite effective. Corresponding to the four load variation scenarios, Table 5 presents fault location estimates with the adopted load compensation technique for locating faults occurring on feeder section 4–7. It is manifested from the results that the fault location accuracy has been considerably improved with the load compensation technique.

Note that the tested system is not a meshed system, and the applicability of the method for meshed systems may be further studied in the future. In addition, performance of the proposed method for cases with non-linear loads and cases with high impedance faults where fault current is comparable to load current requires further research.

4. Conclusions

This paper presents a novel fault location method that is applicable to both radial and non-radial distribution systems using only local measurements. Unbalances and shunt capacitances have been explicitly modeled. The method dispenses with the need for fault type information and offers a direct and generic solution to any type of faults by reducing iterative steps. Simulation studies have evinced that the proposed method yields accurate results and is desirably insensitive to potential measurement errors and load variations.

Besides, although not required for calculating the fault location, the fault type can be obtained as a byproduct thereafter, and may be useful for other fault analysis applications. In case of multiple estimates due to presence of laterals, fake estimates may be eliminated based on fault currents flowing through fault resistances calculated after the fault location is obtained.

References

[1] M.M. Saha, J. Izykowski, E. Rosolowski, Fault Location on Power Networks, Springer-Verlag London Limited, London, 2009.
[2] W.H. Kersting, Distribution System Modeling and Analysis, CRC Press, Taylor & Francis Group, Boca Raton, FL, USA, 2012.
[3] R. Das, M.S. Sachdev, T.S. Sidhu, A fault locator for radial subtransmission and distribution lines, in: IEEE Power Engineering Society Summer Meeting, Seattle, WA, USA, July 16–20, 2000.
[4] H. Li, A. Mokhar, N. Jenkins, Automatic fault location on distribution network using voltage sag measurements, in: The 18th International Conference on Electricity Distribution, Turin, Italy, June 6–9, 2005.
[5] R. Aggarwal, Y. Aslan, A. Johns, New concept in fault location for overhead distribution systems using superimposed components, IEE Proc. – Gener. Transm. Distrib. 144 (May (3)) (1997) 309–316.
[6] R. Pereira, L. Silva, M. Kezunovic, J. Mantovani, Improved fault location on distribution feeders based on matching during-fault voltage sags, IEEE Trans. Power Del. 24 (April (2)) (2009) 852–862.
[7] V.N. Gohokar, M.K. Khedkar, Faults locations in automated distribution system, Electr. Power Syst. Res. 75 (July (1)) (2005) 51–55.
[8] E. Senger, G. Manassero, C. Goldemberg, E. Pellini, Automated fault location system for primary distribution networks, IEEE Trans. Power Del. 20 (April (2)) (2005) 1332–2005.
[9] A.A. Girgis, C.M. Fallon, D.L. Lubkeman, A fault location technique for rural distribution feeders, IEEE Trans. Ind. Appl. 29 (November/December (6)) (1993) 1170–1175.
[10] J. Kim, M. Baran, G. Lampley, Estimation of fault location on distribution feeders using PQ monitoring data, in: IEEE Power Engineering Society General Meeting, Tampa, FL, USA, June 24–28, 2007.
[11] J. Zhu, D. Lubkeman, A. Girgis, Automated fault location and diagnosis and electric power distribution feeders", IEEE Trans. Power Del. 12 (April (2)) (1997) 801–809.
[12] Y. Aslan, Diagnosis of shunt faults in power distribution feeders and laterals, J. Appl. Sci. 5 (9) (2005) 1582–1588.
[13] S.-J. Lee, M.-S. Choi, S.-H. Kang, B.-G. Jin, D.-S. Lee, B.-S. Ahn, N.-S. Yoon, H.-Y. Kim, S.-B. Wee, An intelligent and efficient fault location and diagnosis scheme for radial distribution systems, IEEE Trans. Power Del. 19 (April (2)) (2004) 524–532.
[14] R.H. Salim, M. Resener, A.D. Filomena, K.R. Oliveira, A.S. Bretas, Extended fault-location formulation for power distribution systems, IEEE Trans. Power Del. 24 (April (2)) (2009) 508–516.
[15] M.-S. Choi, S.-J. Lee, S.-I. Lim, D.-S. Lee, X. Yang, A direct three-phase circuit analysis-based fault location for line-to-line fault, IEEE Trans. Power Del. 22 (October (4)) (2007) 2541–2547.
[16] F. Muzi, L. Passacantando, A real-time monitoring and diagnostic procedure for electrical distribution networks, Int. J. Energy 1 (1) (2007) 17–21.
[17] G. Morales-España, J. Mora-Flórez, H. Vargas-Torres, Elimination of multiple estimation for fault location in radial power systems by using fundamental single-end measurements, IEEE Trans. Power Del. 24 (July (3)) (2009) 1382–1389.
[18] Y. Liao, Generalized fault location methods for overhead electric distribution systems, IEEE Trans. Power Del. 26 (January (1)) (2011) 53–64.
[19] R. Krishnathevar, E.E. Ngu, Generalized impedance-based fault location for distribution systems, IEEE Trans. Power Del. 27 (January (1)) (2012) 449–451.
[20] X. Yang, M.-S. Choi, S.-J. Lee, C.-W. Ten, S.-I. Lim, Fault location for underground power cable using distributed parameter approach, IEEE Trans. Power Syst. 23 (November (4)) (2008) 1809–1816.
[21] A.D. Filomena, M. Resener, R.H. Salim, A.S. Bretas, Fault location for underground distribution feeders: an extended impedance-based formulation with capacitive current compensation, Electr. Power Energy Syst. 31 (9) (2009) 489–496.
[22] F.V. Lopes, B.F. Küsel, K.M. Silva, D. Fernandes Jr., W.L.A. Neves, Fault location on transmission lines little longer than half-wavelength, Electr. Power Syst. Res. 114 (September) (2014) 101–109.
[23] A.S. Dobakhshari, A.M. Ranjbar, A closed-form solution for transmission line fault location using local measurements at a remote substation, Electr. Power Syst. Res. 111 (June) (2014) 115–122.
[24] Z. Galijasevic, A. Abur, Fault location using voltage measurements, IEEE Trans. Power Del. 17 (April (2)) (2002) 441–445.
[25] M. Avendaño-Mora, J.V. Milanović, Generalized formulation of the optimal monitor placement problem for fault location, Electr. Power Syst. Res. 93 (December (12)) (2012) 120–126.
[26] C.A. Apostolopoulos, G.N. Korres, A novel algorithm for locating faults on transposed/untransposed transmission lines without utilizing line parameters, IEEE Trans. Power Del. 25 (October (4)) (2010) 2328–2338.
[27] G. Preston, Z.M. Radojevic, C.H. Kim, V. Terzija, New settings-free fault location algorithm based on synchronised sampling, IET Gener. Transm. Distrib. 5 (March (3)) (2011) 376–383.
[28] B. Das, Fuzzy logic-based fault-type identification in unbalanced radial power distribution system, IEEE Trans. Power Del. 21 (January (1)) (2006) 278–285.
[29] Matlab Help Manual, The Mathworks Inc., 2009.
[30] W.H. Kersting, Radial distribution test feeders, in: IEEE Power Engineering Society Winter Meeting, Columbus, Ohio, USA, January 28–February 1, 2001.